

Electron transmission through NiSi_2 -Si interfaces

M. D. Stiles

National Institute of Standards and Technology, Gaithersburg, Maryland 20899

D. R. Hamann

AT&T Bell Laboratories, 600 Mountain Avenue, Murray Hill, New Jersey 07974

(Received 10 May 1989)

Calculations of electron transmission through epitaxial $\text{NiSi}_2/\text{Si}(111)$ interfaces illustrate the versatility of a newly developed first-principles technique. The transmission is poor and very dependent on the interface structure; of the electrons of primary importance for transport, more than 50% are reflected by the type-*A* orientation interface and more than 80% by the type *B*.

INTRODUCTION

Nickel disilicide-silicon (111) interfaces challenge our theoretical understanding of dynamical scattering effects in electron transmission. Their geometries are simple and completely characterized because they are pseudomorphic and atomically abrupt.^{1,2} They can be grown with two relative orientations of the lattices, allowing a test of structural effects on transmission with all other things being held constant. The band lineup is such that there are kinematically allowed states for ballistic transmission to occur, so that inelastic and defect scattering need not dominate the transmission.^{3,4} Using NiSi_2/Si as our example, we report the first realistic calculation of electron transmission probabilities across interfaces between qualitatively dissimilar materials.

These results show the importance of developing a detailed understanding of the transmission properties of interfaces between such different materials. The usefulness of such interfaces in applications depends critically on the transmission properties which cannot be estimated from simplistic models such as the effective-mass approximation. The method we present here is capable of calculating the dependence of the transmission probability on the atomic scale details for interfaces as complicated as $\text{NiSi}_2/\text{Si}(111)$ and demonstrates that models, like the effective-mass approximation, that ignore atomic-scale details will be wrong in many cases. The results we present should be experimentally testable either with device-like structures similar to those⁵ made for $\text{CoSi}_2/\text{Si}(111)$, for which there are not kinematically allowed states for ballistic transmission to occur, or with ballistic electron emission spectroscopy⁶ on thin layers of silicide grown on silicon. Testing these results would either verify that these calculations correctly describe the transmission process or indicate that more work is required to understand it.

Depending on the growth conditions, NiSi_2 grows on $\text{Si}(111)$ surfaces either with the same crystallographic orientation as the Si, called type-*A* growth, or rotated 180° around the interface normal, called type-*B* growth.¹ Experimental structural studies² are consistent with interface structures having a sevenfold-coordinated Ni atom at the interface, denoted *7A* (shown in Fig. 1) and *7B*.

Given a network of bonds across the interface that has essentially undistorted lengths and angles, with only a broken Ni bond, and knowledge that states above the Fermi level are mostly on the Si anyway,³ one might naively expect good electron transmission. In fact, we find that both interfaces strongly reflect electrons, the *7B* structure much more so than the *7A*. This anisotropy is also unexpected, since only third-neighbor coordination changes.

SUMMARY OF METHOD

We have developed a method for calculating the electronic structure of solid systems which are two dimensionally periodic, but of arbitrary structure and infinite extent in the third ("normal" or "*z*") dimension.⁷ The system is divided by planes into a series of layers, as shown in Fig. 1 for the NiSi_2/Si interface. We have a series of identical layers of bulk material *A* (NiSi_2) on the left-hand side, an *A-B* interface layer labeled *C* in the center, and layers of *B* (Si) on the right-hand side. Self-consistent potentials for each layer are obtained from several separate bulk and supercell calculations, and join continuously. We intro-

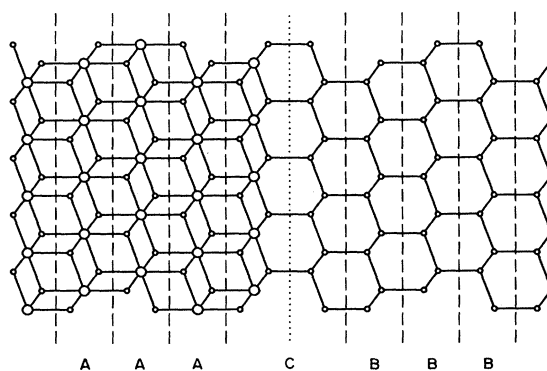


FIG. 1. $[1\bar{1}0]$ projection of the $\text{NiSi}_2/\text{Si}(111)$ interface, showing Si (small) and Ni (large) atoms and near-neighbor bonds. The dashed lines indicate planes dividing the system into three types of layers: bulk NiSi_2 (*A*), bulk Si_2 (*B*), and joining (*C*). The dotted line is discussed in the text.

duce a set of basis functions for each layer which have Bloch periodicity parallel to the layers with a selected parallel wave vector \mathbf{K} . We then vary their coefficients to make a functional of the trial wave function ϕ stationary. The functional

$$J = \frac{1}{2} \int_{\text{cell}} d^3r \{ \phi(\mathbf{r})^* [2m(\hat{H} - E)\phi(\mathbf{r})] + [2m(\hat{H} - E)\phi(\mathbf{r})]^* \phi(\mathbf{r}) \} \\ + \frac{1}{2} \sum_X \int_{\text{IWSC}} d^2R \{ [(\hat{\Lambda} + \hat{\partial}_n)\phi(\mathbf{R}, z_X)]^* \phi(\mathbf{R}, z_X) + \phi(\mathbf{R}, z_X)^* [(\hat{\Lambda} + \hat{\partial}_n)\phi(\mathbf{R}, z_X)] \} \\ - \sum_X \int_{\text{IWSC}} d^2R [t_X(\mathbf{R})^* \phi(\mathbf{R}, z_X) + \phi(\mathbf{R}, z_X)^* t_X(\mathbf{R})], \quad (1)$$

contains a volume term with Hamiltonian \hat{H} , and interface Wigner-Seitz cell (IWSC) boundary terms, in which $\mathbf{r} = (\mathbf{R}, z_X)$, $X = (\text{left}, \text{right})$, $t_X(\mathbf{R})$ is an inhomogeneous term, $\hat{\partial}_n$ is the outward normal derivative, and

$$\hat{\Lambda} = \alpha \left[E_0 - \frac{\partial^2}{\partial R^2} \right]^{1/2}, \quad (2)$$

where α and E_0 are arbitrary.⁸ The variational principle forces the boundary value

$$b_X(\mathbf{R}) = \hat{\Lambda}\phi(\mathbf{R}, z_X) + \hat{\partial}_n\phi(\mathbf{R}, z_X) \quad (3)$$

to converge to the inhomogeneous target values $t_X(\mathbf{R})$, and ϕ to satisfy Schrödinger's equation at energy E , in the limit of a complete basis.^{7,8}

Since the Euler-Lagrange equation for J is linear in ϕ and t_X , we expand t_X in N parallel plane waves $(\mathbf{K} + \mathbf{G})$, and find stationary solutions for the $2N$ t_X 's formed by setting one Fourier component at a time to 1 and the rest to 0 for $X = \text{left}, \text{right}$. We find the corresponding $2N$ $b_X(\mathbf{R})$, and $2N$ complementary boundary values

$$c_X(\mathbf{R}) = \hat{\Lambda}\phi(\mathbf{R}, z_X) - \hat{\partial}_n\phi(\mathbf{R}, z_X), \quad (4)$$

and Fourier-expand them to find b_{XG} and c_{XG} . Algebraically eliminating the set of t_X 's, we express the response of a layer's wave function to its boundary values as a $2N \times 2N$ matrix operator \tilde{S} ,⁷

$$\mathbf{c} = \tilde{S}\mathbf{b}. \quad (5)$$

Having found \tilde{S} for all the layers, we can use value and slope continuity at the interlayer planes to find the desired wave functions for the entire system.⁷

For the transmission problem, the physical boundary conditions on the wave functions are that they approach incident, reflected, and transmitted Bloch waves at $\pm\infty$. To satisfy these conditions in each bulk region, we calculate the $2N$ generalized Bloch states from a linear eigenvalue problem based upon the algebraic requirement that values and slopes on the two sides of a bulk layer be identical within a factor λ , and involving \tilde{S} . The eigenvalues $\lambda = \exp[-i(k_z + i\kappa_z)(z_{\text{left}} - z_{\text{right}})]$ give the normal Bloch wave vector k_z for propagating waves, and the growth or decay rate κ_z for the evanescent waves. Appropriate propagating and decaying waves in both bulk materials are joined through the interface using \tilde{S} for layer C to form the desired scattering states.⁷

We have improved upon the methods we described in Ref. 7 by symmetrizing our approximate \tilde{S} 's according to

a generalized hermiticity condition

$$\tilde{S}\Lambda = \Lambda\tilde{S}^\dagger, \quad (6)$$

which can be shown to be obeyed in the limit of a complete basis. Λ is a diagonal matrix representing the operator $\tilde{\Lambda}$ in Eq. (2). The symmetrized \tilde{S} 's conserve current exactly across each layer, so evanescent waves have identically zero current, and exact matching through the interface layer can replace the constrained least-squares procedure.⁷

We have implemented this approach using linear-augmented-plane-wave eigenfunctions of appropriate bulk and supercell problems as our basis states, and self-consistent local-density-functional potentials in a compatible form.⁹ Interface potentials from the Ni_2Si_8 7A supercell introduced for interface energy calculations,¹⁰ and a similar 7B supercell, were used. Layer C in Fig. 1 constitutes half of the supercell. We tested our programs, and convergence with respect to the basis set,¹¹ as follows.

(1) We compared propagating states from the layer calculations for Si and NiSi_2 with conventionally calculated bands from the same potentials. (2) We compared the transmission with that calculated using a thinner interface layer (dotted line in Fig. 1) formed both by taking a smaller cut of the Ni_2Si_8 supercells and from Ni_2Si_6 supercells. (3) Using the thin C layer, we joined B -oriented Si to an A -supercell C layer, and vice versa. The invariance of the calculated transmission under tests (2) and (3) also indicates that the excellent potential continuity between the bulk layers and our larger C layer (0.001 hartree rms) is not really necessary in this case.

RESULTS

We calculated the transmission of electrons with energies within a few tenths of an eV of the Si conduction-band minimum ($E_c \equiv 0$), since these are the carriers of importance at experimental interfaces. Our supercell potentials and the experimental Si band gap give Schottky barrier heights for the 7A and 7B structures of 0.75 and 0.82 eV, respectively, which are quite close to the experimental values of 0.65 to 0.79 eV.¹² Most of our results were calculated using the band alignments produced by this potential.

Figure 2 shows the transmission through both 7A and 7B interfaces for the \mathbf{K} of the conduction-band minimum (1) and several nearby \mathbf{K} 's (2 and 3). All transmission probabilities are zero at the band minima for each \mathbf{K} , and then increase, initially as the square root of the energy

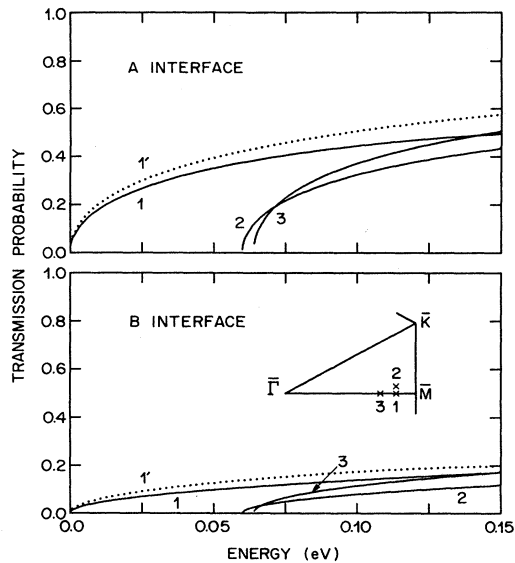


FIG. 2. Electron transmission through $7A$ and $7B$ $\text{NiSi}_2/\text{Si}(111)$ interfaces for three \mathbf{K} 's indicated in the inset Brillouin-zone segment, at energies near the conduction-band minimum. The dotted curve $1'$ is explained in the text.

above the minimum. For an incident energy of 0.15 eV, about 50% of the incident electrons are reflected by the $7A$ interface and 80% by the $7B$ interface. This large difference in the transmission cannot be explained by an effective-mass approximation that ignores the atomic scale details of the wave function. For both interface orientations, the predicted transmission is too weak to make metal-base transistors with useful gain, but such device-like structures could be used to test these predictions of both the strength of the reflection and the difference between the two orientations.

The band alignment between the two bulk materials is incorrect because of the well-known band-gap problem of the density functional method. In spite of this problem, the close match between the resulting wave functions and the quasiparticle wave functions found using the nonlocal self-energy^{13,14} indicate that the main correction to our results would be due to the incorrect band alignment. Since determining the actual self-energy operators for these interface systems is far beyond present computational capabilities, we have simulated them by adding a smoothly varying potential to the interface layer to give the experimental conduction-band-Fermi-level alignment. The resulting transmission, shown by the dotted lines in Fig. 2, shows very little difference from the unshifted case. This invariance depends on the fact that the band structure in the NiSi_2 does not change much over the relevant energy range: if there were band extrema in this range, any change in the lineup would make a big difference. The difference between the transmission for the two orientations is thus a robust result, not dependent on the small Schottky-barrier height difference, (as established by the tests described in the previous section of this paper) or on self-energy corrections.

We determined, using least-squares wave function

matching through the shorter joining region, that the minimal model that could reproduce our results required at least seven states. These states include the incident, reflected, and transmitted states and the two most rapidly decaying evanescent states with the proper symmetry from each bulk; using just the propagating states gives qualitative errors, as was found previously for silicon twist boundaries.⁷ This gives an indication of why an effective-mass approximation will not work for these systems.

To help understand the difference between the electron states for $7A$ and $7B$, we produced contour plots of probability and normal-flux densities on the "interface plane" (Si side, dotted line in Fig. 1) and on the NiSi_2 side of the joining layer. The plots for the electron incident from Si are more informative, and are shown in Fig. 3 for the $7A$ and $7B$ structures for \mathbf{K} at the band minimum, and $E = 0.1$ eV. We kept \mathbf{K} fixed in NiSi_2 and the joining layer, so \mathbf{K} switches to another of the six conduction-band minima when we rotate the Si from $7A$ to $7B$. Since \mathbf{K} lies in a mirror symmetry plane and the incident state is even, only even states couple in. (The lines where the mirror planes intersect the plots are perpendicular to the tilted edges, running through the obtuse vertices on the Si side, and through the centers of the rhombi on the NiSi_2 side.)

The incident (\mathcal{I}) state for $A(B)$ and the reflected (\mathcal{R}) state for $B(A)$ are identical except for a flux reversal because of the valley switch. The flux flows in tubes for these states, with significant cancellation, so each \mathcal{I} matches its \mathcal{R} reasonably well, which promotes reflection.⁷ The total wave functions on the Si side ($\mathcal{I} + \mathcal{R} + \text{evanescents}$) are not qualitatively changed from $\mathcal{I} + \mathcal{R}$ (except for some canceling flux for B) so the

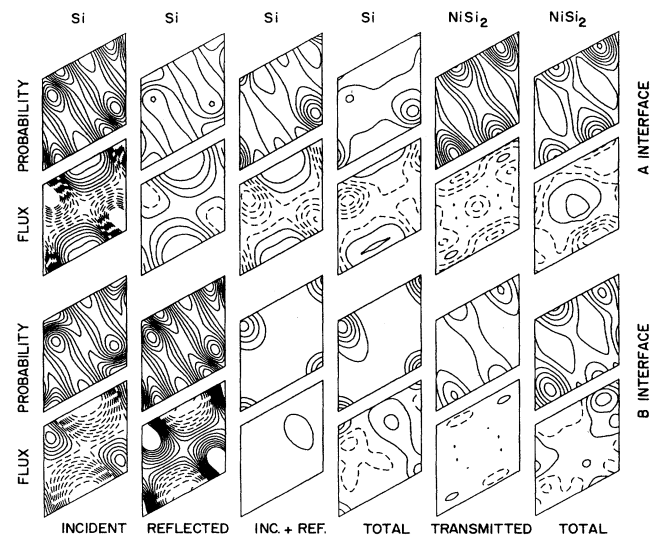


FIG. 3. Probability and flux density plots for two scattering states on the Si and NiSi_2 sides of the "thin" joining region (see text). Interface-normal bonds intersect the plotting plane at the vertices of the Si rhombi, and at points $\frac{1}{6}$ and $\frac{5}{6}$ along the long diagonal of the NiSi_2 rhombi. Probability density contours are spaced by 1.25×10^{-4} a.u. and flux density contours by 5.0×10^{-5} a.u. Dashed contours are negative.

evanescent do not play too large a role here. The probability densities are highest near the bonds, but slightly offset in opposite directions for A and B . The transmitted (T) state has almost all its flux in one direction, suggesting a mismatch to \mathcal{J} . Of course the potential is quite different on this plane, so this suggestion has limited validity. Comparing T to total on the NiSi_2 side shows that the evanescent play a much larger role for B than A . These total probability densities are also peaked along the bonds, but along the bond from a Si atom in the interface triple layer for A , and from a Ni for B . It is tempting to speculate that it is harder to propagate current through the incompletely bonded Ni than the fully bonded Si, and

that the $\mathcal{J}\mathcal{R}$ phase changes producing this shift in weight lead to the A - B transmission difference.

SUMMARY

Using a realistic calculation, we have shown that $\text{NiSi}_2/\text{Si}(111)$ interfaces are strongly reflecting and that there is a strong orientation dependence to the transmission probability. Experimentally verifying these results would confirm our ability to calculate the electronic properties of such interfaces and allow us to apply our methods with confidence to other interfaces of interest.

¹R. T. Tung, J. M. Gibson, and J. M. Poate, *Phys. Rev. Lett.* **50**, 429 (1983).

²D. Cherns, G. R. Antis, J. L. Hutchinson, and J. C. H. Spence, *Philos. Mag. A* **46**, 849 (1982); E. Vlieg, A. E. M. J. Fischer, J. F. van der Veen, B. N. Dev, and G. Materlik, *Surf. Sci.* **178**, 36 (1986); E. J. van Loenen, J. W. M. Frenken, J. F. van der Veen, and S. Valeri, *Phys. Rev. Lett.* **54**, 827 (1985).

³Y. J. Chabal, D. R. Hamann, J. E. Rowe, and M. Schlüter, *Phys. Rev. B* **25**, 7598 (1982); D. M. Bylander, L. Kleinman, K. Mednick, and W. R. Grise, *ibid.* **26**, 6379 (1982).

⁴For $\text{CoSi}_2/\text{Si}(111)$, there are no kinematically allowed CoSi_2 bands near the Si conduction-band minimum, so ballistic transmission cannot occur. L. F. Mattheiss and D. R. Hamann, *Phys. Rev. B* **37**, 623 (1988).

⁵A. F. J. Levi, R. T. Tung, J. L. Batstone, and M. Anzlowar, in *Silicon on Insulators and Buried Metals in Semiconductors*, edited by J. C. Sturm, C. K. Chen, L. Pfeiffer, and P. L. F. Hemment, Materials Research Society Symposia Proceedings, Vol. 107 (Materials Research Society, Pittsburgh, 1988), p. 259.

⁶W. J. Kaiser and L. D. Bell, *Phys. Rev. Lett.* **60**, 1406 (1988); L. D. Bell and W. J. Kaiser, *ibid.* **61**, 2368 (1988).

⁷M. D. Stiles and D. R. Hamann, *Phys. Rev. B* **38**, 2021 (1988).

⁸G. Wachutka, *Phys. Rev. B* **34**, 8512 (1986).

⁹L. F. Mattheiss and D. R. Hamann, *Phys. Rev. B* **33**, 823 (1986).

¹⁰D. R. Hamann, *Phys. Rev. Lett.* **60**, 313 (1988).

¹¹For the LAPW's, we used $l_{\text{max}}=8, 6$, and 10 in the Ni, Si, and cut Si muffin tins, $|\mathbf{k}+\mathbf{g}|^2 < 15$ a.u. [$\mathbf{k}, \mathbf{g}=(\mathbf{K}, k_z), \mathbf{G}, g_z$]], and $|\mathbf{K}+\mathbf{G}|^2 < 10.5$ a.u. For the potential and cut muffin-tin projector, we used $l_{\text{max}}=6, 6$, and 12, in the Ni, Si, and cut Si muffin tins, $|\mathbf{g}|^2 < 70$ a.u. for the bulk interstitial regions, and $|\mathbf{G}|^2 < 70$, $g_z^2 < 5600$ a.u. for the cut supercell interstitial region. For the basis sets, we used 150 (300) eigenfunctions per k_z and 2 (1) k_z 's for the bulk (interface) layers. For the generalized Bloch states and layer matching, we used $|\mathbf{K}+\mathbf{G}|^2 < 6.5$ a.u.

¹²R. T. Tung, *Phys. Rev. Lett.* **52**, 462 (1984); *J. Vac. Sci. Technol. B* **2**, 465 (1984).

¹³M. S. Hybertsen and S. G. Louie, *Phys. Rev. Lett.* **55**, 1418 (1985); *Phys. Rev. B* **34**, 5390 (1986).

¹⁴R. W. Godby, M. Schlüter, and L. J. Sham, *Phys. Rev. Lett.* **56**, 2415 (1986); *Phys. Rev. B* **35**, 4170 (1987).